

# 1,2-Bis(methylsulfonyl)-1-(2-chloroethyl)-2-[[1-(4-nitrophenyl)ethoxy]carbonyl]hydrazine (KS119): a Cytotoxic Prodrug with Two Stable Conformations Differing in Biological and Physical Properties

Philip G. Penketh<sup>1,\*</sup>, Raymond P. Baumann<sup>1</sup>, Krishnamurthy Shyam<sup>1</sup>, Hugh S. Williamson<sup>2</sup>, Kimiko Ishiguro<sup>1</sup>, Rui Zhu<sup>1</sup>, Emma S. E. Eriksson<sup>3</sup>, Leif A. Eriksson<sup>3</sup> and Alan C. Sartorelli<sup>1</sup>

<sup>1</sup>Department of Pharmacology, Yale University School of Medicine, New Haven, CT 06520, USA

<sup>2</sup>BP Exploration, Chertsey Road, Sunbury-on-Thames, Middlesex, TW16 7LN, UK

<sup>3</sup>School of Chemistry, National University of Ireland – Galway, University Road, Galway, Ireland

\*Corresponding author: Philip G. Penketh, philip.penketh@yale.edu or philip.penketh@gmail.com

**The anticancer prodrug 1,2-bis(methylsulfonyl)-1-(2-chloroethyl)-2-[[1-(4-nitrophenyl)ethoxy]carbonyl]hydrazine (KS119) selectively releases a short-lived cytotoxin following enzymatic reduction in hypoxic environments found in solid tumors. KS119, in addition to two enantiomers, has two stable atropisomers (conformers differing in structure owing to hindered bond rotation) that interconvert at 37 °C in aqueous solution by first-order kinetics with  $t_{1/2}$  values of ~50 and ~64 h. The atropisomers differ in physical properties such as partition coefficients that allow their chromatographic separation on non-chiral columns. A striking difference in the rate of metabolism of the two atropisomers occurs in intact EMT6 murine mammary carcinoma cells under oxygen-deficient conditions. A structurally related molecule, 1,2-bis(methylsulfonyl)-1-(2-chloroethyl)-2-[[1-(3-hydroxy-4-nitrophenyl)ethoxy]carbonyl]hydrazine (KS119WOH), was also found to exist in similar stable atropisomers. The ratio of the atropisomers of KS119 and structurally related agents has the potential to impact the bioavailability, activation, and therapeutic activity. Thus, thermally stable atropisomers/conformers in small molecules can result in chemically and enantiomerically pure compounds having differences in biological activities.**

**Key words:** atropisomers, chemotherapy, conformers, cytotoxicity, hypoxia, KS119, prodrug, targeting

**Abbreviations:** 90CE, 1,2-bis(methylsulfonyl)-1-(2-chloroethyl)hydrazine; CIP, calf intestinal alkaline phosphatase; DPP, differential pulse polarography;  $E_{1/2}$ , polarographic half-wave reduction potential; G-C ethane cross-link, 1-(N<sup>3</sup>-cytosinyl)-2-(N<sup>1</sup>-guaninyl)ethane; KS119, 1,2-bis(methylsulfonyl)-1-(2-chloroethyl)-2-[[1-(4-nitrophenyl)ethoxy]carbonyl]hydrazine; KS119W, 1,2-bis(methylsulfonyl)-1-(2-chloroethyl)-2-[[1-(3-phospho-4-nitrophenyl)ethoxy]carbonyl]hydrazine; KS119WOH, 1,2-bis(methylsulfonyl)-1-(2-chloroethyl)-2-[[1-(3-hydroxy-4-nitrophenyl)ethoxy]carbonyl]hydrazine; PNBC, 1,2-bis(methylsulfonyl)-1-(2-chloroethyl)-2-[[4-nitrobenzyloxy]carbonyl]hydrazine.

Received 7 January 2011, revised 12 July 2011 and accepted for publication 14 July 2011

1,2-bis(methylsulfonyl)-1-(2-chloroethyl)-2-[[1-(4-nitrophenyl)ethoxy]carbonyl]hydrazine (KS119) is a prodrug that requires an oxygen-deficient reductive environment to liberate a cytotoxin within malignant tumors (1). To accomplish this, KS119 and related molecules are composed of three domains: a 'trigger' region consisting of a nitrobenzyl moiety, an oxycarbonyl 'linker' region, and a cytotoxic 1,2-bis(methylsulfonyl)-1-(2-chloroethyl)hydrazine DNA inter-strand cross-linking agent (90CE) which is considered the 'therapeutic warhead' region (Figure 1) (1,2). 1,2-Bis(methylsulfonyl)-1-(2-chloroethyl)-2-[[1-(4-nitrophenyl)ethoxy]carbonyl]hydrazine was designed to exploit the fact that hypoxic/anoxic areas are found in solid tumors (Figure 1). These oxygen-deficient regions often confound conventional therapeutic strategies involving radiation and chemotherapeutic agents, because the low oxygen tension in solid tumors renders these cells highly resistant to x-irradiation and the poor blood supply to these tumor areas can result in decreased delivery to and activity of cytotoxic drugs at these malignant sites (3–6). In addition, the low oxygen concentration of these cells also encourages metastatic spread (7). These unfavorable properties from a therapeutic point of view are, however, counterbalanced by the fact that oxygen-deficient regions can be exploited to gain specificity by the design of reductively activated prodrugs (1,2,8).

The agents that we are developing, after an initial one electron reduction by enzymes, such as NADPH:cytochrome P450 reductase, NADH:cytochrome b5 reductase and xanthine oxidase, to yield a nitro radical anion, are readily reoxidized by molecular oxygen back

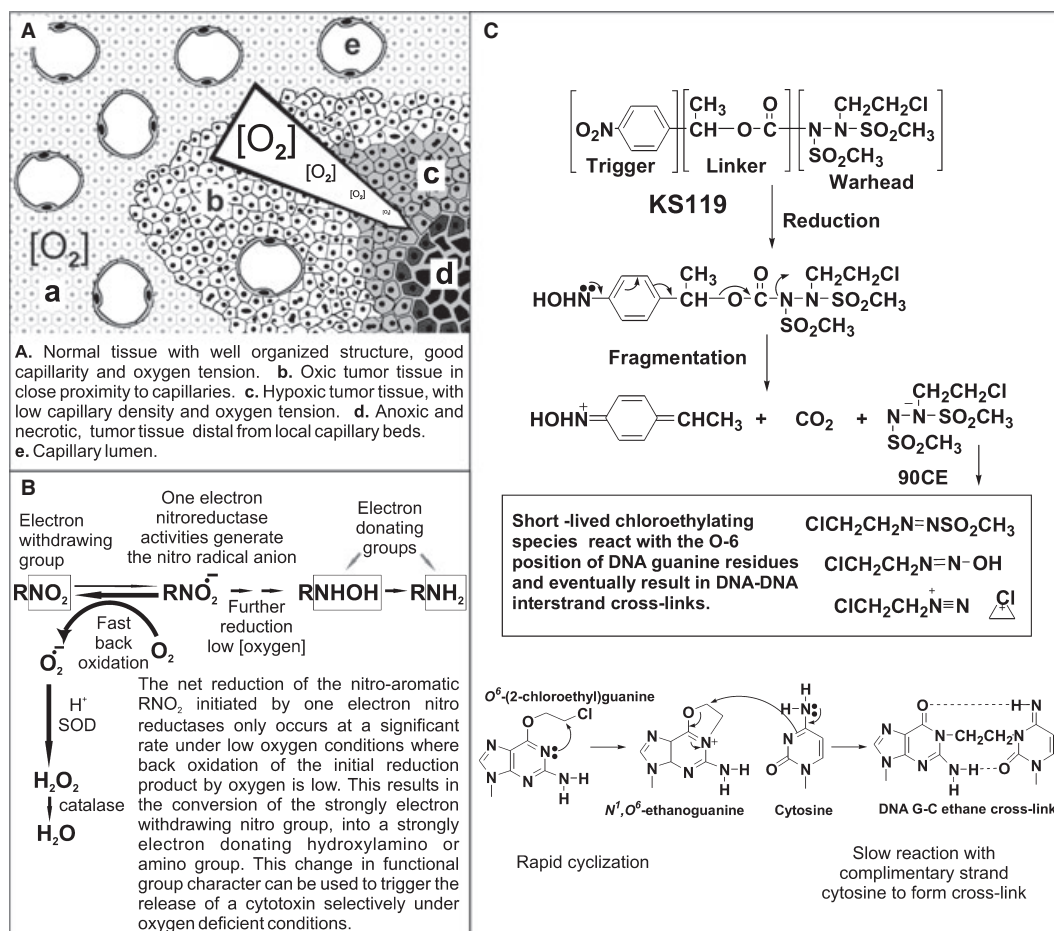


**Figure 1:** Background summarization figure: (A) The distribution of capillaries and oxygen in different regions of a solid tumor and normal tissue. (B) The mechanism underlying the inverse oxygen concentration dependence of net KS119 reduction. (C) The mechanism of fragmentation to generate a chloroethylating species upon reduction and the subsequent formation of a G-C ethane cross-link in DNA by these species.

to the parental drug (Figure 1), thereby protecting normoxic normal tissue. However, upon further reduction of the nitro radical anion to either the amino or hydroxylamino functionality, which only occurs efficiently when the oxygen concentration is low, the molecule relatively rapidly fragments to release the 'therapeutic warhead', a short-lived ( $t_{1/2} = \sim 30$  seconds, at pH 7.4 and 37 °C) alkylating species (90CE) that ultimately results in the formation of a highly toxic DNA G-C ethane interstrand cross-link (1,2,9,10). The short half-life of 90CE permits little diffusional escape to normal tissue, and thus, the bulk of the alkylations are delivered close to the site of parental drug reduction.

1,2-Bis(methylsulfonyl)-1-(2-chloroethyl)-2-[[1-(4-nitrophenyl)ethoxy]carbonyl]hydrazine is a modified version of 1,2-bis(methylsulfonyl)-1-(2-chloroethyl)-2-[[4-nitrobenzyloxy]carbonyl]hydrazine (PNBC), a structurally related agent of lower hypoxic selectivity (1,2). PNBC lacks the shielding methyl group on the methylene carbon adjacent to the linker region (Figure 2) and as such, in addition to reductive activation, is subject to an additional activation mechanism via an  $S_N2$  nucleophilic attack by glutathione/glutathione-S-transferase at

the methylene carbon, resulting in the release of the cytotoxic moiety in the absence of reduction (1,2). The addition of the shielding methyl group of KS119 blocked this secondary mode of activation, thereby increasing the hypoxic selectivity and contributing at least in part to the five log hypoxic/oxic cell kill differential against EMT6 carcinoma cells *in vitro*, previously observed with KS119 (2).

The addition of the methyl group in the linker region introduces a chiral center resulting in two KS119 optical isomers. Surprisingly, the addition of the methyl group also results in significant changes in the polarographic properties of the molecule and the existence of two peaks by HPLC analysis over extended elution times on a non-chiral C18 reverse-phase column (Figure 3). Because such columns (non-chiral) are incapable of separating optical isomers, other structural features must be responsible for this behavior. Our studies indicate that two major distinct and stable conformational forms or atropisomers (conformers differing in structure owing to hindered bond rotation) of KS119 exist (Figure 4) which possess different physical and biological properties.

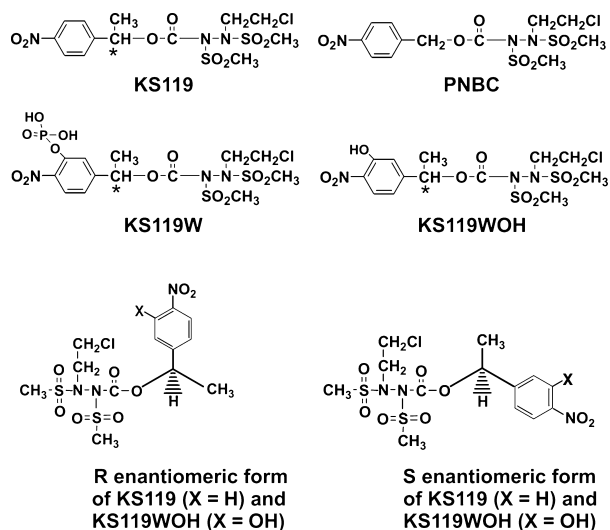


**Figure 2:** Chemical structures of PNBC, KS119, KS119W, and KS119WOH, and the chiral carbon configurations in KS119-R, KS119WOH-R, KS119-S, and KS119WOH-S.

In this study, we have examined the thermal interconversion of the KS119 conformers/atropisomers, their octanol:buffer partition coefficients, their polarographic reduction and their metabolism by NADPH:cytochrome P450 reductase, xanthine oxidase, and EMT6 carcinoma cells under oxygenated and oxygen deficient conditions. The possible therapeutic implications of these conformational differences are discussed.

## Materials and Methods

### Chemicals and reagents

1,2-Bis(methylsulfonyl)-1-(2-chloroethyl)-2-[[1-(4-nitrophenyl)ethoxy]carbonyl]hydrazine (racemic mixture) and PNBC were synthesized as previously described (1). Enantiomerically pure KS119-R and KS119-S were produced by chiral synthesis from their respective chiral nitrobenzyl alcohols by Vion Pharmaceuticals Inc. (New Haven, CT, USA) and were supplied by the company in very limited quantities. KS119W, 1,2-bis(methylsulfonyl)-1-(2-chloroethyl)-2-[[1-(3-phospho-4-nitrophenyl)ethoxy]carbonyl]hydrazine (enantiomers and racemic mixtures) were also provided by Vion Pharmaceuticals. KS119WOH, 1,2-bis(methylsulfonyl)-1-(2-chloroethyl)-2-[[1-(3-hydroxy-4-nitrophenyl)ethoxy]carbonyl]hydrazine (enantiomers and racemic mixtures) were produced in solution immediately prior to HPLC analysis and separation, from KS119W (enantiomers and racemic mixtures) by the enzymatic removal of the phosphate group using calf intestinal alkaline phosphatase (CIP) from New England Biolabs, Ipswich, MA, USA. Briefly, 50  $\mu$ L of 10 mM KS119W dissolved in DMSO was added to 0.95 mL of 50 mM NaCl, 25 mM Tris-HCl, 5 mM MgCl<sub>2</sub>, 0.5 mM dithiothreitol, pH 7.9 buffer containing 20 units of CIP. This mixture was then incubated at 37 °C for 20 min, and stored on ice until used. The aforesaid agents were all greater than 95% purity by HPLC analysis. All other chemicals were purchased from the Sigma-Aldrich Chemical Company, St Louis, MO, USA.

### Determination of KS119 and KS119WOH by HPLC

HPLC measurements of the concentration of KS119 were performed using a Beckman 127P solvent module and a Beckman 168 UV/vis detector (Beckman, Fullerton, CA, USA); two HPLC methods were used. A standard curve for the estimation of total KS119 was established by analyzing known concentrations of KS119 over a range of 0–200  $\mu$ M, and a linear relationship between concentration and the area under the curve was established. The first method (method A) was used to determine the concentration of KS119 conformers when relatively rapid analysis was required. Samples in 30% v/v acetonitrile were separated on a five micron 220  $\times$  4.6 mm Applied Biosystems RP-18 C-18 reverse phase column (Applied Biosystems, Carlsbad, CA, USA) by elution with 34% acetonitrile in buffer (0.03 M KH<sub>2</sub>PO<sub>4</sub>, 1.0 mM NaN<sub>3</sub>, pH 5.4) for 5 min followed by a 34–70% acetonitrile linear gradient in buffer, at a flow rate of 0.6 mL/min from 5 to 35 min. After this point, the concentration of acetonitrile was maintained at this level for 5 min then returned to the starting concentration over an additional 5 min. Absorbance was monitored at 280 nm using a Beckman 168 UV/vis detector. KS119 eluted as a split peak at approximately 35 min. KS119WOH eluted as a split peak at approximately 32 min. To more accurately resolve the proportions of the different conformers and for separation purposes, a second method was developed (method B) by eluting the column with a solvent of constant composition consisting of ~39% acetonitrile and buffer, at a flow rate of 0.6 mL/min. Under these conditions, the conformers of KS119 eluted as two partly overlapping peaks at approximately 83 and 86 min, while the conformers of KS119WOH eluted as two partly overlapping peaks at approximately 69 and 73 min.

### Separation of conformers

Relatively pure samples of the early- and late-eluting conformers of both KS119 and KS119WOH were obtained at purities of >98% by collecting fractions from HPLC (method B) corresponding to the initial rising portion of the early peak and the falling portion of the late peak (Figure 5). The concentration and purity of the conformer preparations were then determined by repeat HPLC. For partition studies, these samples were diluted fourfold with 100 mM potassium phosphate, pH 7.4, and were stored at 0 °C or lower prior to use. This gives aqueous buffer conformer solutions which contain approximately 9.5% acetonitrile and 82 mM potassium phosphate, with the pH value remaining at about 7.3–7.4.

### Preparation of purified KS119A and KS119B for polarographic and cell cytotoxicity studies

To prepare conformer samples for cytotoxicity studies, the conformers were separated as described earlier (HPLC, method B) except that the eluting solutions contained no buffer components or NaN<sub>3</sub>, and consisted of equivalent mixtures of acetonitrile and distilled water. The fractions corresponding to the early- and late-eluting conformers were collected and diluted threefold with ice-cold distilled water, then shaken with 5% by volume of dichloromethane. The mixture was allowed to separate and the lower dichloromethane layer containing the conformers was then collected. The dichloromethane layer was evaporated in an ice bath with a stream of dry nitrogen gas and the residual material dissolved in a small

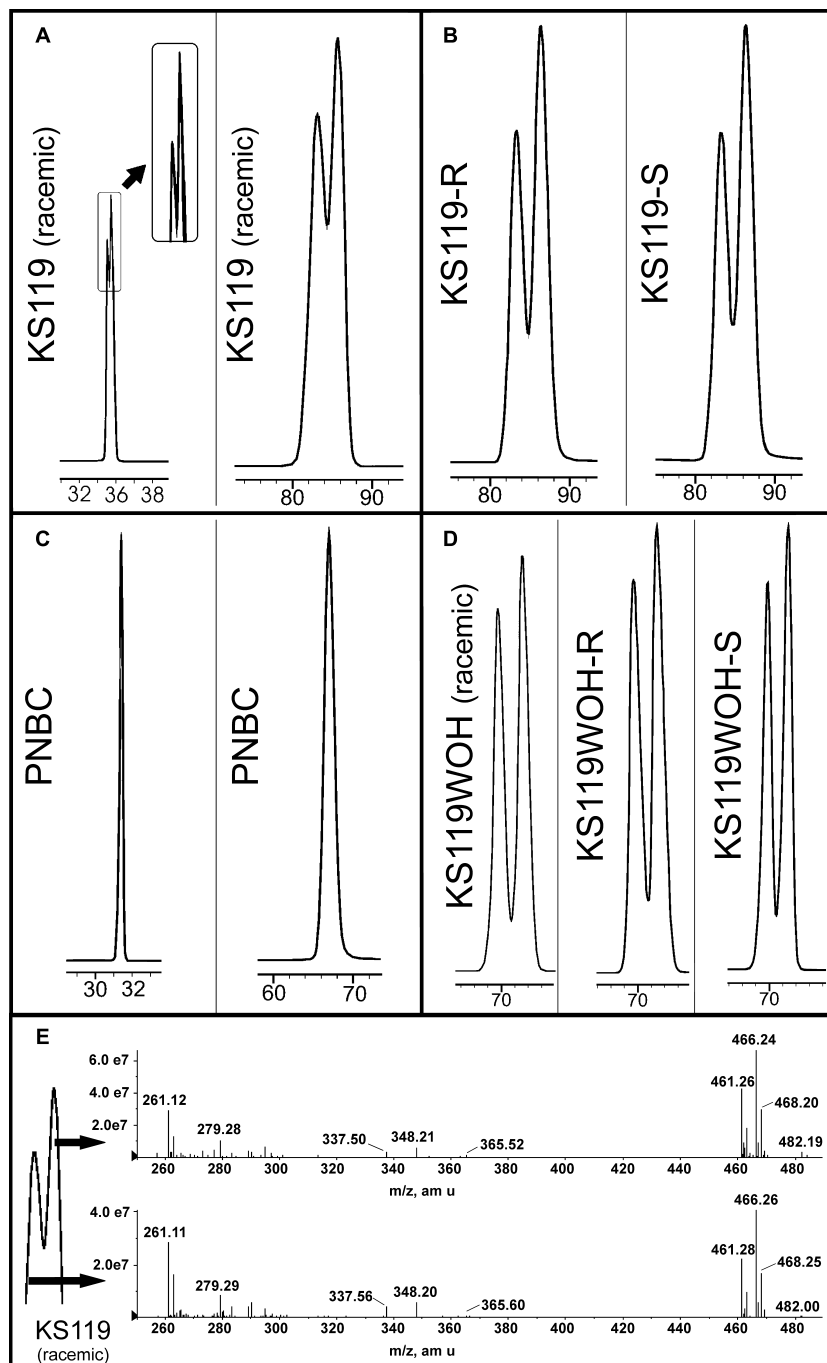


**Figure 3:** HPLC traces of PNBC, KS119, KS119W, and KS119WOH under two different HPLC protocols; fast elution protocol (30–36-min elution time) and slow elution protocol (69–86-min elution time) and LCMS of KS119. Panel A, HPLC traces of (left panel) KS119 (racemic mixture) using the fast elution protocol; (right panel) KS119 (racemic mixture) using the slow elution protocol. Panel B, HPLC traces of KS119 optical isomers using the slow elution protocol (left panel) KS119-R; (right panel) KS119-S. Panel C, HPLC traces of PNBC using the fast elution protocol (left panel); PNBC using the slow elution protocol (right panel). Panel D, HPLC traces of KS119WOH racemic mixture and separate optical isomers using the slow elution protocol (left panel) KS119WOH (racemic mixture); KS119WOH-R (central panel), and KS119WOH-S (right panel). Panel E, LCMS of the early (KS119A)- and late (KS119B)-eluting peaks of KS119 (racemic mixture).

volume of a 70:30 DMSO/water mixture (freezing point  $-70^{\circ}\text{C}$ ) and stored at  $-20^{\circ}\text{C}$  until required. The concentration and purity of the conformer preparations were checked by repeat HPLC prior to use. Conformer preparations stored in this manner maintained a high level of purity ( $>90\%$ ) for greater than a month.

#### LCMS of KS119A and KS119B

Material comprising the rising portion of the early (KS119A) peak and the falling portion of the late (KS119B) peak was analyzed by

mass spectroscopy using a chromatographic system consisting of an Agilent 1200 series HPLC system, including a binary pump (Model G1312B), a vacuum degasser (Model G1379B), an autosampler (Model G1367C), and a column oven (Model G1316B). The mass spectrometer was an Applied Biosystems Sciex 4000 Q-trap<sup>®</sup> mass spectrometer (Applied Biosystems Sciex, Foster, CA, USA). Data acquisition was carried out by ANALYST 1.4.2<sup>®</sup> software on a DELL computer. A declustering potential of 50 V, excitation energy of 100 V and a collision energy of 10 V were utilized.

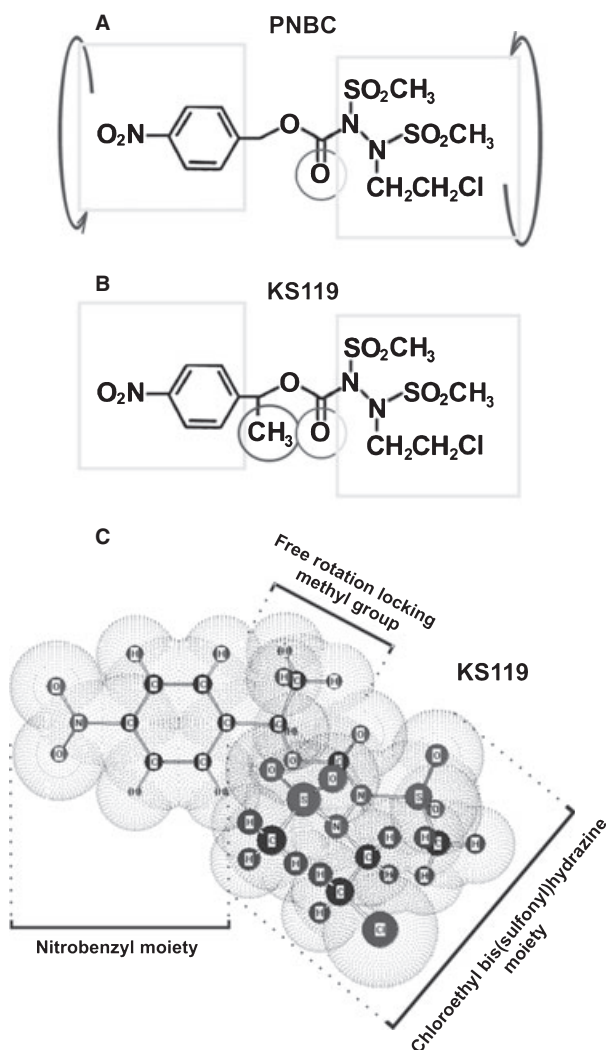


**Figure 4:** Scheme proposed to account for the existence of stable conformers of KS119 but not of PNBC based upon rotational restriction in the linker region. (A) Two-dimensional planar representation scheme showing relatively free rotation of the nitrobenzyl trigger domain with respect to the 1,2-bis(sulfonyl)-1-(2-chloroethyl)hydrazine warhead domain in PNBC. (B) Two-dimensional planar representation scheme showing restricted rotation of the nitrobenzyl trigger domain with respect to the 1,2-bis(sulfonyl)-1-(2-chloroethyl)hydrazine warhead domain in KS119 confining the molecule to particular relative orientations. (C) Space filling three-dimensional representation showing the locking action of the methyl group on the free rotation of the nitrobenzyl trigger domain with respect to the 1,2-bis(sulfonyl)-1-(2-chloroethyl)hydrazine warhead domain in KS119.

#### **Hydrolysis of KS119A and KS119B**

Ten microlitre samples of 5 mM purified KS119A or KS119B solutions (concentration determined by HPLC assuming both conformers have the same extinction at 280 nm as the equilibrium mixture) were added to 990  $\mu$ L of 10 mM NaOH to give 50  $\mu$ M solutions. These solutions were then heated at 100  $^{\circ}$ C for 30 min in sealed

tubes to completely hydrolyze the KS119. The samples were then diluted with an equal volume of 100 mM  $\text{KH}_2\text{PO}_4$  solution. The resultant solutions, containing the equivalent of 25  $\mu$ M hydrolyzed KS119 conformers were then analyzed using HPLC protocol A and compared with an authentic 25  $\mu$ M solution of the 1-(4-nitrophenyl)ethanol synthesized as previously described (1). A sharp peak at  $\sim$ 12 min corresponding to the expected generation of the 1-(4-nitrophenyl)ethanol was observed with both KS119A and KS119B.

#### ***n*-Octanol:buffer partition coefficient determination for conformers of KS119 and KS119WOH**

To determine the octanol:buffer partition coefficients, 20  $\mu$ L of *n*-octanol was added to a 1 mL volume of purified conformer of known concentration determined by HPLC in ice-cold 82 mM potassium phosphate buffer containing 9.5% acetonitrile, pH  $\sim$ 7.4. This mixture was vortexed for 30 seconds and then placed on ice for 30 additional sec, and the process was repeated three times. This mixture was then centrifuged at 10 000 *g* for 30 seconds to separate the phases, and the lower aqueous phase was analyzed by HPLC method A to determine the remaining conformer concentration. From the decrease in conformer concentration in the aqueous phase, and the known volumes of the phases, the partition coefficient was calculated. A much smaller volume of octanol compared with the aqueous phase was used as the KS119 and KS119WOH conformers greatly favored the octanol phase; therefore, for accurate measurement by this method, the concentration in the aqueous phase must not be reduced more than several fold.

#### **Polarographic determination of half-wave reduction potentials**

Differential pulse polarography (DPP) voltgrams of PNBC, KS119, KS119A, and KS119B were obtained using a pH 7.0 buffer composed of 100 mM potassium chloride and 50 mM potassium phosphate as the supporting electrolyte. Compounds were added as 2 mM solutions in DMSO or in 70:30 DMSO/water mixture to give final concentrations of 20  $\mu$ M. The samples were purged with nitrogen to remove dissolved oxygen, and DPP voltgrams were obtained using a Princeton Applied Research electrochemical trace analyzer model 394, linked to a model 303A static mercury drop electrode (Princeton Applied Research, Oak Ridge, TN, USA). Scans were performed from 0 to  $-900$  mV (2 mV/second) using a platinum counter electrode versus an Ag/AgCl reference electrode (saturated KCl/AgCl electrolyte). A pulse amplitude of 50 mV was used and the polarographic half-wave reduction potential  $E_{1/2}$  was calculated from the peak current potential ( $E_p$ ) according to the following equation;  $E_{1/2} = E_p - \text{pulse amplitude}/2$  (11).

#### **Hypoxic/oxic reduction of KS119 conformers by NADPH:cytochrome P450 reductase and xanthine oxidase**

In these experiments, oxygen deficiency was enzymatically generated as previously described (12). Briefly, glucose/glucose oxidase

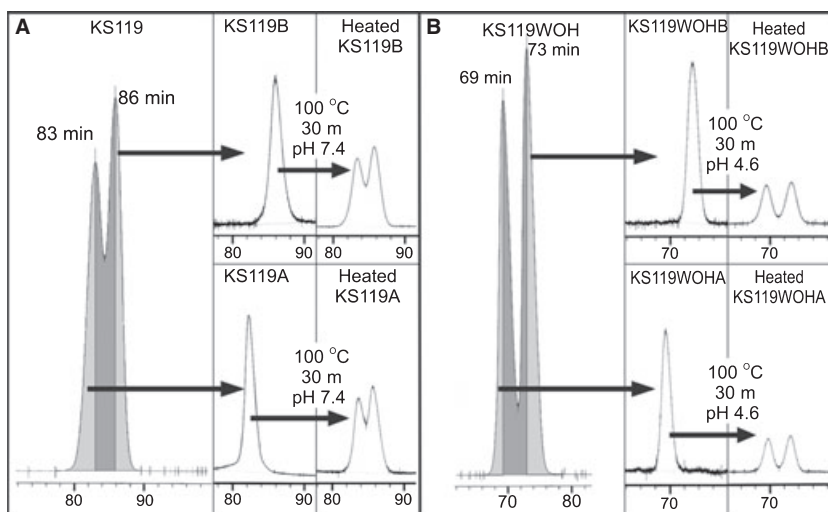


**Figure 5:** Separation/purification of the early- and late-eluting conformers of KS119 and KS119WOH and their thermal re-equilibration. Panel A (left panel) HPLC of racemic KS119 showing the collected fractions corresponding to the initial rising portion of the early-eluting conformer peak and the falling portion of the late-eluting conformer peak. The upper and lower central panels of panel A show the purity of the collected late KS119B and early KS119A eluting conformer fractions, respectively. The upper and lower right hand panels of panel A show the thermal equilibration of the collected pure KS119B and KS119A conformer fractions, respectively, to give the equilibrium mixture of conformers. Panel B (left panel) HPLC of racemic KS119WOH showing the collected fractions corresponding to the initial rising portion of the early-eluting conformer KS119WOHA peak and the falling portion of the late-eluting conformer KS119WOHB peak. The upper and lower central panels of panel B show the purity of the collected KS119WOHB and KS119WOHA conformer fractions, respectively. The upper and lower right hand panels of panel B show the thermal equilibration of the collected pure KS119WOHB and KS119WOHA eluting conformer fractions, respectively, to give the equilibrium mixture of conformers.

was used to rapidly consume the available free oxygen, and catalase was employed to remove generated hydrogen peroxide. In the absence of other components, this system itself does not measurably reduce KS119 in the time frames employed in these experiments. The reaction mixtures in a total volume of 0.5 mL were as follows: 100 mM potassium phosphate buffer, pH 7.4, containing 10 mM glucose, 5  $\mu$ L of a solution of glucose oxidase (200 units/mL) and catalase (12 000 units/mL), 20  $\mu$ M KS119 (added as a 100 $\times$  solution in DMSO) plus either 5  $\mu$ L of 104 units/mL of NADPH:cytochrome P450 reductase (Sigma, human recombinant C8113) plus 1 mM NADPH or 0.16 units/mL of xanthine oxidase (Sigma, bovine milk, X4500-5UN) plus 1 mM xanthine. The aerobic reactions were identical except that the glucose needed for the oxygen deficiency system to operate was omitted. Furthermore, the aerobic reaction volumes were scaled up 10-fold and the mixture incubated as a shallow layer with shaking in sealed T25 culture flasks to ensure that full air saturation was maintained and evaporation prevented. The reaction mixtures were incubated at 37  $^{\circ}$ C and samples were removed at 0, 1, 2 and 3 h after initiation, mixed with an equal volume of CH<sub>3</sub>CN and centrifuged at 10 000 *g* for 10 min to sediment any precipitated protein. The supernatant was then analyzed using HPLC method A for KS119 content and conformer composition.

#### Reduction of KS119 by EMT6 cells

These experiments were performed in a manner similar to the enzymatic studies. They involved following the time course of the loss

of the conformers of KS119, when 20  $\mu$ M KS119, consisting of the normal equilibrium mixture of conformers, was incubated under oxygenated conditions (shaken in a shallow layer in T25 flasks) and oxygen-deficient conditions (0.7 mL aliquots in microfuge tubes plus the enzymes required to create oxygen deficient conditions) with 10<sup>7</sup> EMT6 carcinoma cells/mL for 3 h in Dulbecco's Minimal Essential Medium (DMEM) supplemented with 10% fetal bovine serum and 10 mM glucose. At 0, 1, 2 and 3 h, aliquots were mixed with an equal volume of acetonitrile, in which KS119 is very soluble, to quench the enzymatic reactions, lyse the cells, precipitate the enzymes and other macromolecules and extract the remaining KS119. These samples were allowed to stand at room temperature for 15 min to complete the precipitation then centrifuged at 10 000 *g* for 10 min. The supernatant was then analyzed using HPLC method A.

#### Clonogenic cytotoxicity assays

Clonogenic survival assays were performed essentially as described previously (13). O<sup>6</sup>-Alkylguanine-DNA alkyltransferase-deficient EMT6 tumor cells were seeded into 25-cm<sup>2</sup> plastic tissue culture flasks at 5–8  $\times$  10<sup>5</sup> cells per flask. When confluent, cells were treated with either the early (KS119A)- or late (KS119B)-eluting conformer of KS119 dissolved in 70% v/v DMSO aqueous mixture in a total volume of 10 mL of medium for 4 h at 37  $^{\circ}$ C. For oxygen-deficient conditions, cells were incubated with KS119 conformers in the presence of 2 units/mL of glucose oxidase (Sigma G6641), 120 units/mL of catalase (Sigma, C1345) in high glucose Dulbecco's

modified Eagle medium (Invitrogen, Carlsbad, CA, USA). Flasks were flushed with nitrogen for 10 seconds and caps were screwed on tightly. This facilitates oxygen depletion of the medium by glucose oxidase through the removal of residual oxygen containing air and denial of the entry of additional air. After a 4-h treatment, monolayers were rinsed, and cells were detached by trypsinization, suspended in culture medium, counted and sequential cell dilutions were plated in duplicate into 6-well plates at a density of  $1 \times 10^2$ ,  $1 \times 10^3$ , and  $1 \times 10^4$  cells per well. Ten days later, colonies were fixed, stained with 0.25% crystal violet in 80% methanol and quantified. All analyses were corrected for plating efficiency in the presence of the DMSO vehicle at concentrations equivalent to those used for exposure to the test agent. DMSO concentrations were  $\leq 0.5\%$  and non-toxic. In the absence of cells, no measurable direct metabolism of KS119 was detected in the presence of the glucose oxidase and catalase enzyme components of the oxygen deficiency generating system (12).

### Computational methodology for molecular conformation prediction

A range of conformations of KS119S corresponding to different energy minima were geometry-optimized using the M06 functional (14) in combination with the 6-311 + G(2d,2p) basis set. The geometry optimizations were performed in aqueous bulk solvent modeled using the C-PCM formalism (15,16). This is the implementation of the conductor-like screening model COSMO (17) in the PCM framework, with atomic radii optimized for COSMO-RS. Frequency calculations were performed at the same level of theory in bulk solvation and it was confirmed that the optimized geometries correspond to energy minima (no imaginary frequencies). In the evaluation of data, the correction to the Gibbs free energy at 298 K was added to the minimum energies in solvent. All calculations were carried out in the GAUSSIAN 09 program (18).

## Results

### HPLC analysis of KS119

HPLC analysis of samples of chemically pure KS119 by elemental analyses, while giving a single peak under short elution time conditions (<15 min), gave a split peak under extended elution times (35 min), and two partially overlapping peaks (at 83 and 86 min) under relatively long elution times. The two components had relative peak areas of approximately 43 and 57 for the earlier eluting (KS119A) and later eluting (KS119B) components, respectively (Figure 3). Material from the rising portion of the early peak and the falling portion of the late peak was analyzed by mass spectroscopy. The resulting mass spectra recorded for KS119A and KS119B were essentially identical and contained the expected KS119 molecular ion sodium adduct peak of 466.25 (443.25 + 23), confirming the chemical equivalence of these two components (Figure 3).

Pure samples of PNBC synthesized in an identical manner, except for the use of 4-nitrobenzyl alcohol in place of 1-(4-nitrophenyl)ethanol as a starting material, gave a single peak in all cases using identical HPLC conditions (Figure 3).

### Confirmation of equivalent absorbancies at 280 nm

Purified samples of KS119A and KS119B quantified by HPLC, assuming that both forms had extinction coefficients at 280 nm that were identical to the KS119 equilibrium mixture standard, were subjected to alkaline hydrolysis and both forms gave essentially identical molar yields of 1-(4-nitrophenyl)ethanol. The measured yields of 1-(4-nitrophenyl)ethanol from KS119A and KS119B were  $100 \pm 2\%$  and  $98 \pm 2\%$ , respectively. These findings verified the assumption that both forms have equivalent or very close to equivalent optical absorbancies at 280 nm. Therefore, the relative HPLC peak areas at 280 nm directly correspond to the relative quantities of the two forms.

### HPLC analysis of pure KS119 optical isomers

The addition of the methyl group in KS119 to the methylene carbon within the linker region introduces a chiral center, resulting in two optical isomers. Very small quantities of enantiomerically pure optical isomers of KS119 synthesized from their respective enantiomerically pure chiral alcohols supplied by Vion Pharmaceuticals Inc. were analyzed under identical HPLC conditions. Both the R and S isomers of KS119 gave identical, two peak, HPLC traces indistinguishable from that produced by the racemic mixture (Figure 3). HPLC traces of the racemic mixture, enantiomerically pure R-form and enantiomerically pure S-form KS119WOH also gave equivalent double peak HPLC traces (Figure 3).

### Thermal equilibration

Purified KS119A, KS119B, KS119WOHA, and KS119WOHB were heated in dilute solution. This resulted in the purified components re-establishing the two peak HPLC pattern previously observed under the appropriate conditions (Figure 5). Thus, heating either KS119A or KS119B for 30 min at 100 °C gave the equilibrium ratio of KS119A:KS119B of approximately 43–57 regardless of the initial concentration in the range tested (1–50  $\mu\text{M}$ ). This heat treatment was too intense for the less chemically stable KS119WOH, as it resulted in the complete decomposition of this compound. The pH was decreased from  $\sim 7.4$  to 4.6 to chemically stabilize KS119WOH and the experiment repeated. Equilibration of KS119WOHA and KS119WOHB (the early- and late-eluting forms of KS119WOH, respectively) was then observed with an approximate 45% loss of material because of chemical decomposition. A study of the interconversion of the conformers at physiologically relevant temperatures and pH values was then undertaken. These studies involved incubating the purified KS119A and KS119B in a largely aqueous buffer of 82 mM potassium phosphate, pH  $\sim 7.4$  at 37 °C, for periods of up to 10 days and following the proportions of each form by HPLC; under these conditions, approximately 28–30 h were required to reach the half equilibrium point in the case of KS119. The low chemical stability of KS119WOH under these conditions complicated the experiments which were not further pursued in detail; however, the kinetics for the interconversion of the KS119WOH conformers appeared to be similar to those of KS119. Time points from six separate KS119 equilibration experiments (three each for the conversion of KS119A to KS119A/KS119B equilibrium mixture and KS119B to KS119A/KS119B equilibrium mixture) were combined

into a single figure (Figure 6) and compared with calculated curves. These curves were derived from equations describing the concentration of KS119A and KS119B versus time, starting with pure KS119A or pure KS119B, and assuming the conversion of KS119A to KS119B and KS119B to KS119A were both first-order processes. The first-order rate constants can be calculated from the time required to reach the half equilibrium point. At pH  $\sim$ 7.4 and 37 °C, the calculated first-order rate constants  $K_a$  and  $K_b$  were approximately 0.33 and 0.26/day, respectively; these values corresponded to half lives of 50.4 h for KS119A and 64 h for KS119B. To obtain approximate values for the activation energies for these transitions, using the Arrhenius equation, a similar series of experiments were performed at 65 °C where half lives of 1.7 h for KS119A and 2.3 h for KS119B were calculated (first-order rate constants  $K_a$  and  $K_b$  were approximately 0.4 and 0.3/h, respectively, at 65 °C). Activation energies of  $\sim$ 103 and  $\sim$ 105 kJ/mol were calculated for the KS119A to KS119B and KS119B to KS119A reactions, respectively. From the equilibrium position, we determined the  $\Delta G^\circ$  under the reaction conditions employed for the KS119A to KS119B conversion to be  $-0.73$  kJ/mol.

### Partition coefficient differences between conformers

The octanol:buffer partition coefficients were determined for KS119A and KS119B and values of  $139.9 \pm 1.2$  (SEM) and  $159.4 \pm 1.8$  (SEM), respectively, were obtained. A proportionally larger difference was found in the partition coefficients of KS119WOHA and KS119WOHB of  $20.4 \pm 0.8$  (SEM) and  $24.2 \pm 0.9$  (SEM), respectively.

### Comparison of the half-wave reduction potentials ( $E_{1/2}$ ) of KS119 conformers and PNBC

Differential pulse polarography (DPP) voltgrams of PNBC and KS119 were also recorded; PNBC gave a single peak corresponding to a  $E_{1/2}$  of about  $-453$  mV, while two peaks were observed in the case of KS119, corresponding to  $E_{1/2}$  values of approximately  $-415$  and  $-575$  mV (Figure 7). Both purified conformers gave almost identical two peak traces.

### Relative conformer enzymic reduction rates

To determine whether the conformers of KS119 differed substantially in their rates of reduction by two commonly used nitro reductase enzymes, NADPH:cytochrome P450 reductase and xanthine oxidase, equilibrium mixtures of the conformers were incubated with each enzyme system under oxygen-deficient conditions, and samples were withdrawn at various time intervals and analyzed by HPLC. Even at time points at which the total KS119 was largely consumed, no significant changes were observed in the ratios of the conformers in the remaining KS119 (Figure 8).

### Relative conformer reduction rates by intact EMT6 cells

The conformer preference of intact EMT6 tumor cells under oxygenated and oxygen-deficient conditions was also studied. This cell line has a high level of total nitro reductase activity. Under oxygen-deficient conditions, net KS119 loss occurred at  $\sim$ 3.3 $\times$  the oxygenated

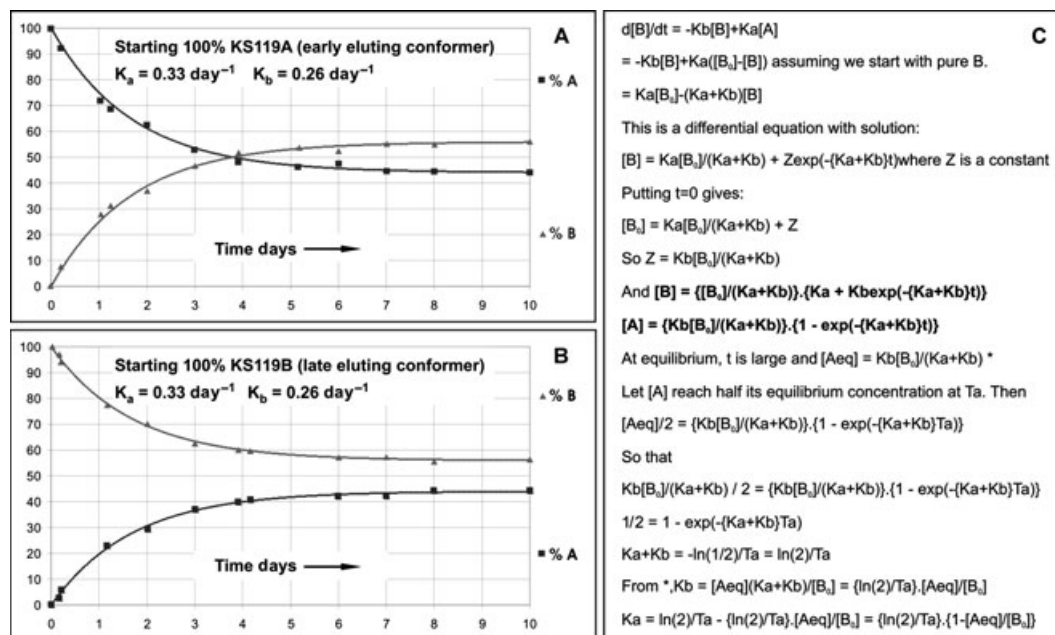


**Figure 6:** Calculated KS119 conformer proportion curves versus time at 37 °C assuming first-order kinetics for the interconversion of the conformers ( $K_a = 0.33$ /day and  $K_b = 0.26$ /day corresponding to  $t_{1/2}$  values of 50.4 and 64 h for KS119A and KS119B, respectively) starting with 100% KS119A conformer (early-eluting conformer) panel A, and 100% KS119B conformer (late-eluting conformer) panel B. Experimental points from six experiments (three starting with 100% KS119A and three experiments starting with 100% KS119B) are overlaid on these calculated curves. Panel C, derivation of expressions for the concentrations of KS119A (A) and KS119B (B) versus time (starting with 100% KS119B) and  $K_a$  from the half equilibrium time.

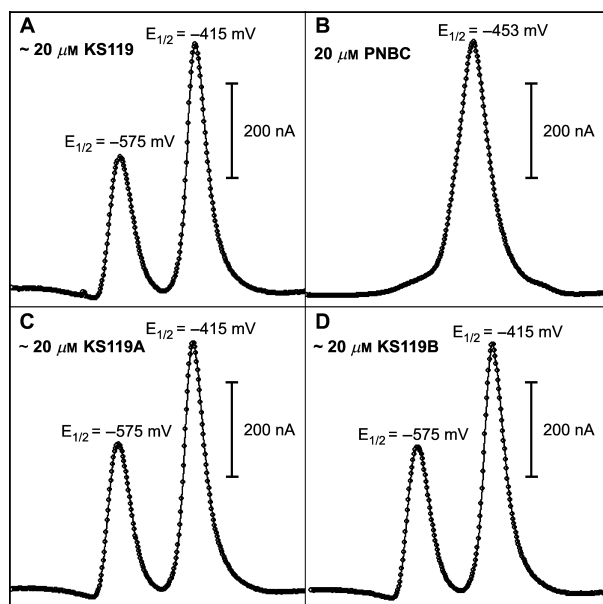


**Figure 7:** Differential pulse polarograms of KS119 and PNBC. Panel A, differential pulse polarogram of an equilibrium mixture of KS119. Panel B, differential pulse polarogram of PNBC. Panel C, differential pulse polarogram of KS119A (early-eluting conformer). Panel D, differential pulse polarogram of KS119B (late-eluting conformer).

rate, with a strong preference for the late-eluting KS119B conformer over the KS119A conformer (Figure 9). The starting KS119A:KS119B ratio was approximately 0.75, but after 3 h under oxygen-deficient conditions with  $10^7$  EMT6 cells/mL this ratio increased to 3.25. Under oxygenated conditions, a preference for

the KS119B conformer was also suggested, with the conformer ratio increasing slightly to 0.80 over 3 h.

### Relative cytotoxicity of KS119A and KS119B toward EMT6 cells under oxygen-deficient conditions

The cytotoxicities of the purified conformers against EMT6 cells were measured in a clonal assay after a relatively short period of drug exposure (4 h) to minimize problems of equilibration. These experiments indicated that the more avidly reduced KS119B conformer was more cytotoxic than the less readily reduced KS119A conformer (Figure 10).

### Computational chemistry-based conformations

Figure 11 displays two out of several conformations found for KS119S. These two conformations display the largest differences in structure (open/closed) and likely display the largest differences in physical properties. Several other conformations corresponding to additional energy minima on the potential energy surface were also found, with energies between these two extreme cases.

### Discussion

HPLC traces of pure KS119 displayed two peaks under slow elution conditions (Figure 3). This was not observed with PNBC, a molecule differing only by the absence of the methyl group that produces the chiral center (Figure 2). Non-chiral columns, such as the C18 reverse-phase column used, are incapable of separating optical isomers (19); therefore, features not solely relating to the chiral carbon must be responsible. This was confirmed by HPLC of the pure optical isomers, both of which gave two peak traces identical to the

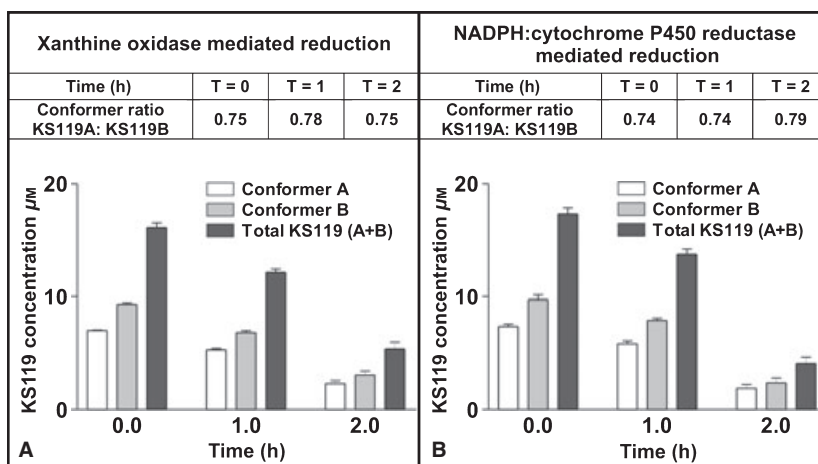


**Figure 8:** The reduction of KS119 and lack of conformer preference exhibited by xanthine oxidase and NADPH:cytochrome P450 reductase under oxygen-deficient conditions. Panel A, reduction of total KS119 and the contributions of KS119A (early-eluting conformer) and KS119B (late-eluting conformer) to the total versus time by xanthine oxidase under oxygen-deficient conditions. The concentration ratio of the conformers at the different time points is given in the included table. Panel B, reduction of total KS119 and the contributions of KS119A (early-eluting conformer) and KS119B (late-eluting conformer) to the total versus time by NADPH:cytochrome P450 reductase under oxygen-deficient conditions. The concentration ratio of the conformers at the different time points is given in the included table.

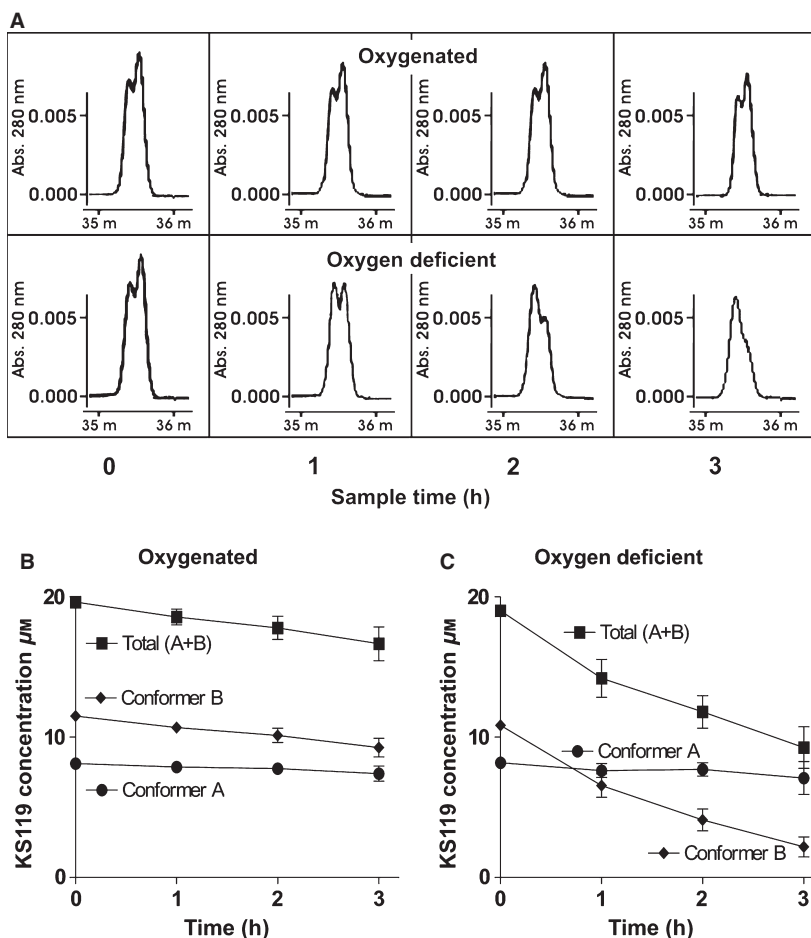


**Figure 9:** Conformer selective metabolism of KS119 by EMT6 carcinoma cells. Panel A, upper row shows typical HPLC traces of samples taken from oxygenated incubations of  $20 \mu\text{M}$  KS119 with EMT6 cells at  $10^7$  cells/mL at 0, 1, 2 and 3 h; lower row shows typical HPLC traces of samples taken from oxygen-deficient incubations of  $20 \mu\text{M}$  KS119 with EMT6 cells at  $10^7$  cells/mL at 0, 1, 2, and 3 h. Panels B and C are graphical representations of the data in panel A. Panel B, plots of the concentrations (mean of three experiments) of total KS119 (initial concentration  $\sim 20 \mu\text{M}$ ) and the contributions of KS119A (early-eluting conformer) and KS119B (late-eluting conformer) to the total versus time under oxygenated conditions during incubations with EMT6 cells at  $10^7$  cells/mL. Panel C, plots of the concentrations (mean of three experiments) of total KS119 (initial concentration  $\sim 20 \mu\text{M}$ ) and the contributions of KS119A (early-eluting conformer) and KS119B (late-eluting conformer) to the total versus time under oxygen-deficient conditions during incubations with EMT6 cells at  $10^7$  cells/mL.

racemic mixture (Figure 3). Identical phenomena were observed with the optical isomers and the racemic mixture of a related molecule, KS119WOH (Figure 3). LCMS gave identical mass spectra for KS119A and KS119B confirming their equivalent composition and that the two peaks were not a consequence of the reversible formation of an unanticipated covalent adduct with a solvent or buffer component. Furthermore, purified KS119A and KS119B thermally re-equilibrated at moderate temperatures (Figure 5). This could not occur with chiral carbon-based optical isomers of the structure type present in KS119 and KS119WOH. If equilibration was possible, a 50:50 rather than a 43:57 ratio would result, as optical isomers have identical thermodynamic properties (20). The kinetics of equilibration closely matched our model, which assumes that both components interconvert with first-order kinetics, with half-lives at  $37^\circ\text{C}$  and pH 7.4 of 50.4 and 64 h for KS119A and KS119B, respectively (Figure 6).

The chemical stability of KS119 and KS119WOH is partly dependent upon the electron withdrawing effects of the nitro group; reduction to an electron-donating group results in molecular fragmentation (Figure 1) (1). The phenolic hydroxyl group in KS119WOH exists largely as an anion at physiological pH, with the negative charge being delocalized to the nitro group attenuating its stabilizing actions. At pH 7.4 and  $37^\circ\text{C}$ , the chemical half-life of KS119WOH is less than that for the conformational interconversions. Dropping the pH to 4.6 stabilizes KS119WOH sufficiently to observe conformational equilibration (Figure 5).

Space filling molecular models of PNBC allow free rotation of the nitrobenzyl and chloroethyl bis(sulfonyl)hydrazine moieties with respect to each other and the linker domain, whereas in models of KS119, it is more hindered because of the steric interference produced by the bulky methyl group in the linker region (Figure 4). This

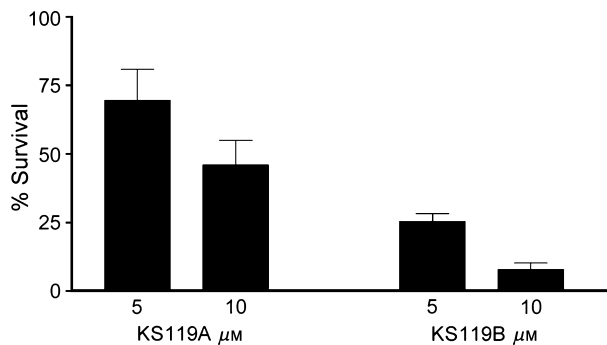


**Figure 10:** Cytotoxicity of KS119A and KS119B to EMT6 carcinoma cells after a 4-h exposure under conditions of oxygen deficiency. Cells were treated with either 0, 5, or 10  $\mu\text{M}$  KS119A or KS119B conformer in medium for 4 h at 37  $^{\circ}\text{C}$  under conditions of oxygen deficiency. After 4 h of treatment, the cells were washed free of agent, detached by trypsinization, and plated at densities of  $1 \times 10^2$ ,  $1 \times 10^3$ , and  $1 \times 10^4$  cells per well. Ten days later, colonies were quantified and the surviving percentage calculated. The data represent the arithmetic means of three experiments  $\pm$  the standard error values.

may help confine KS119 to two major spatial conformations or atropisomers. Atropisomers are usually the consequence of hindered rotation around a bond because of the presence of bulky neighboring substituents and or the bond possessing partial double bond character. To be defined as an atropisomer, the conformational forms must have half-lives of greater than 1000 seconds under ambient conditions (21–23). Atropisomerism is becoming an emerging problem for the pharmaceutical industry as examples with half-lives as long as 1000 years, differing in biological activity by hundreds of fold have been discovered (24,25). The consequences of hindered rotation can be somewhat similar to traditional chiral centers and can give rise to geometrical diastereoisomers which have different physical properties. Symmetrization can be used to eliminate chiral axes (as well as chiral centers) and diastereoisomeric atropisomers can be frequently prevented using this strategy (24). A loss of diastereoisomeric atropisomerism as a consequence of symmetrization probably explains the single HPLC peak observed for PNBC. Peptide type bonds can have partial double bond character owing to the lone electron pair on the amino group being delocalized to the carbonyl group; this produces two possible conformations corresponding to cis and trans isomers (26). In KS119, a carbonyl group is attached to a hydrazine nitrogen and a

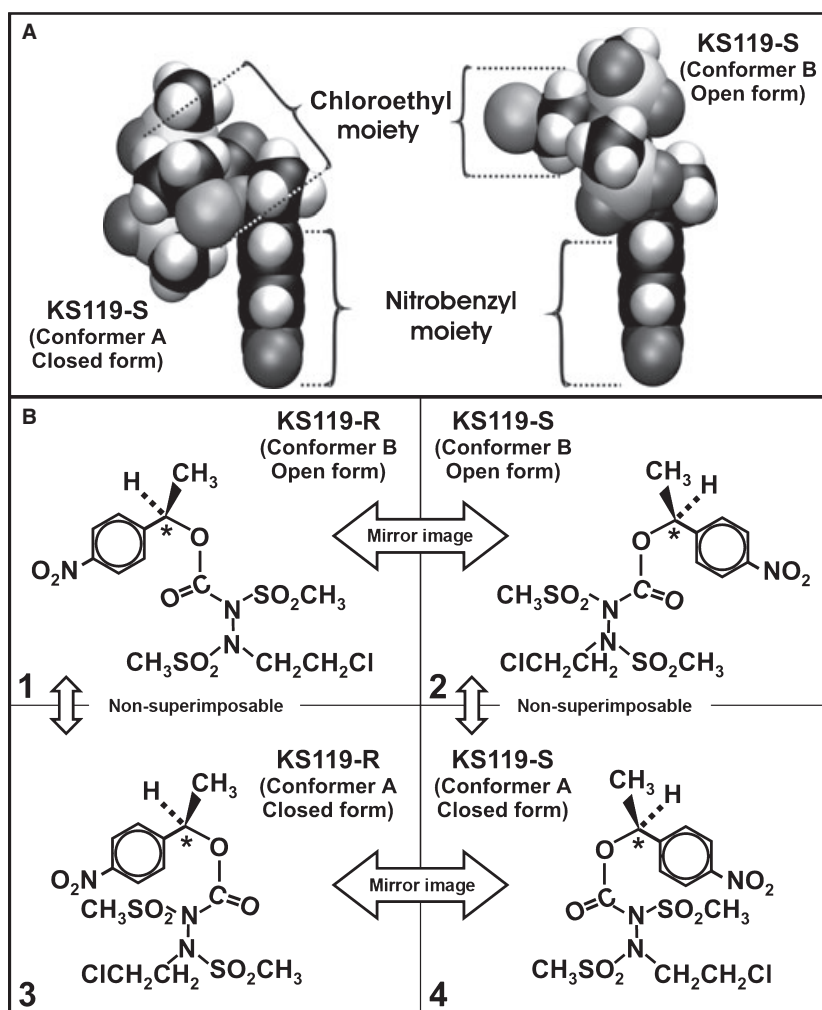


**Figure 11:** Computer-predicted open and closed conformations of KS119 and schematic representing the different KS119 forms and conformations. Panel A, computer-predicted three-dimensional conformations of the open and closed forms of KS119S corresponding to calculated stable energy minima. Panel B, Schematic of the four forms of KS119 indicating the mirror image pairs (1,2) and (3,4) with identical physical properties and the non-superimposable pairs (1,3) and (2,4) with dissimilar physical properties.

similar situation could be envisioned resulting in restricted rotation at this bond. However, unlike the peptide bond case, the nitrogen lone pair is not freely available for delocalization to the carbonyl oxygen because of a highly electron withdrawing methylsulfonyl neighboring group. An illustration of this effect is the fact that the N–H group in 90CE is a weak acid (9) rather than being basic. The bond attaching the oxygen to the opposite side of the carbonyl group with respect to the nitrogen has the potential to exhibit partial double bond character because of electron lone pair delocalization, permitting two stable axial configurations which could give rise to diastereoisomeric atropisomers in the case of KS119. In this case, the electron-deficient nitrogen would promote this effect. We have performed some computer-based conformational modeling consistent with this hypothesis. Two out of several predicted conformations were of particular interest as these conformations displayed the largest differences in stable structure (open/closed) which would likely result in measurable differences in partition and HPLC behavior. Other conformations corresponding to additional energy minima on the potential energy surface were also found, with energies and structure in-between the two favored predictions. These calculated open/closed conformations are illustrated in Figure 11, together with a graphic illustrating how a KS119 racemic mixture and both its pure R and S forms could all appear to be mixtures of molecules with the same two sets of dissimilar physical properties. Although additional stabilization because of partial double bond character is not possible at the N–N bond of the hydrazine moiety, making conformational forms at this position less likely, sterically restricted bond rotation because of the presence of four bulky substituents could still be possible, resulting in diastereoisomeric atropisomers because of the presence of the chiral carbon in KS119. If the two forms represented an equilibrium between slowly dissociating dimers and slowly associating monomers, the equilibrium position would be expected to change with concentration rather than be fixed, and only the dissociation would be expected to show first-order kinetics. Furthermore, upon heating, dissociation would be likely, resulting in an increase in monomer concentration, rather than a re-equilibration. A much larger HPLC separation would also be expected. Therefore, we believe the two distinct forms of KS119 are atropisomers arising purely because of the large activation energy of  $\sim 100$  kJ/mol required to circumvent steric/electronic hindrance barriers to rotation probably around the oxygen to carbonyl moiety bond. X-Ray crystallography of the purified atropisomers may be required to determine unambiguously the precise structural differences between these forms.

Differences in the octanol:buffer partition coefficients of approximately 14% and 19% were measured for the conformers of KS119 and KS119WOH, respectively. The proportionally greater difference in the partition coefficients of KS119WOH conformers probably explains their superior HPLC separation. These differences must reflect a change in the relative solvent exposed hydrophilic and hydrophobic surface areas between the two conformations and would be consistent with the computer-predicted forms, with KS119A and KS119B corresponding to the closed and open structures, respectively. Such differences also mean that the equilibrium position would be somewhat dependent on the solvent (something we have observed); furthermore, if the transition state involved a change in the exposed hydrophobic areas, the activation energy for

the transition would also be influenced by the solvent. As the octanol:water partition coefficient has a major influence on absorption, distribution, target binding, metabolism, and excretion, conformers would exhibit some differences in biological activity *in vivo* purely from these differences. The influence of the octanol:water partition coefficient on the therapeutic index of nitrosourea alkylating agents has been reported and the nitrosoureas with the greatest partition coefficients tended to have the greatest therapeutic indices (27).

The DPP voltogram of PNBC gave a single peak corresponding to an  $E_{1/2}$  of  $-453$  mV, whereas that of KS119 gave two peaks corresponding to  $E_{1/2}$  values of approximately  $-415$  and  $-575$  mV (Figure 7). Initially, we suspected that these two peaks corresponded to the two conformations, with the large difference in their  $E_{1/2}$  values being because of the nitro groups being in very different local environments. However, this did not appear to be the case, as both purified conformers of KS119 gave almost identical two peak traces. The  $E_{1/2}$  values of approximately  $-415$  and  $-453$  mV undoubtedly correspond to the reduction of the nitro group of KS119 and PNBC, respectively. The additional peak ( $E_{1/2} -575$  mV) seen with KS119 is not the expected consequence of the addition of an electrochemically inert methyl group on the linker region, but could correspond to the reduction of a linker component favored by steric strain.

The enzymes NADPH:cytochrome P450 reductase and xanthine oxidase did not appear to differ in their KS119 conformer preference. Even when the total KS119 was largely consumed, no significant change in the ratio of the conformers in the residual KS119 was seen (Figure 8). This contrasts sharply with the EMT6 cell experiments where a strong preference (>sevenfold) for KS119B was observed. The starting KS119A:KS119B ratio was approximately 0.75, but after 3 h under oxygen-deficient conditions, this ratio increased to 3.25 compared to 0.80 under oxygenated conditions, where the net metabolism was much less because of back oxidation. Several factors may be involved in this preference: (i) selective uptake of KS119B or export of KS119A, leading to a greater concentration of KS119B within the cell and increased enzymatic reduction/metabolism, (ii) selective enzymatic reduction of the KS119B; even though xanthine oxidase and NADPH:cytochrome P450 reductase showed no real conformer preference, other reducing systems with conformer preference might be operative, or (iii) a combination of these effects. If these agents entered cells solely by passive diffusion, the more hydrophobic KS119B would be expected to enter cells somewhat faster than KS119A and this could account for at least a portion of the selectivity.

A mechanism involving the direct conversion of KS119B to KS119A by the cell is thought to be unlikely, as the ratio changed little under oxygenated conditions when there was little net metabolism. The concentration and ratio changes appear to be consistent with the preferential loss of KS119B. The preferential reductive activation of KS119B would be expected to result in KS119B expressing more cytotoxicity than KS119A. Therefore, we measured the cytotoxicity of EMT6 cells of the purified conformers in a clonal assay (Figure 10). It is clear that KS119B is significantly more cytotoxic than KS119A; this difference is particularly apparent at the highest concentrations. Based upon the conformer preference observed in

Figure 9, one might have expected to see an even larger difference in the relative cytotoxicities. However, these two experimental procedures have important differences; in the conformer preference experiment, the conformers are competing for metabolism/uptake, whereas in the differential cytotoxicity experiments, the cells were exposed to each purified individual conformer in the absence of a competitor. If uptake/metabolism of both conformers occurred by the same proteins, it is likely that the uptake/metabolism of the less preferred KS119A would be greater in the absence of competing KS119B, leading to a smaller fold differential in experiments where the conformers were tested individually. Furthermore, some degree of equilibration of the conformers will occur in these experiments, resulting in a smaller differential.

## Conclusions and Future Directions

The unusually high stability (half-life >2 days at physiological pH and temperature) of the two conformational forms/atropisomers of KS119 allowed them to be treated and characterized as two distinct compounds with differing physical and biological properties. Thus, manipulation of the conformer ratio could conceivably have therapeutic benefits. For example, enrichment for KS119B may increase potency if KS119 was normally cleared rapidly. Alternatively, enriching for the more poorly metabolized KS119A may provide more time for distribution into oxygen-deficient regions where eventual equilibration could generate the more potent KS119B.

The role of different three-dimensional conformations in simple molecules is not usually given much consideration, largely because of the normally rapid free rotation around single bonds and the lack of strong stabilizing interactions between different regions of small molecules precludes stable energy minima at normal temperatures. While KS119 may represent an unusual case, the present work supports the earlier findings of other examples of stable conformations with different biological activities in relatively small molecules (24). In the case of KS119, small differences in their chromatographic properties alerted us to their presence; however, atropisomers/conformers could occur in other small molecules without readily discernible differences in chromatographic properties under many conditions. Thus, atropisomers/conformers could go largely undetected despite potentially having large differences in their biological properties that may contribute toward experimental variability or biphasic/multiphasic responses.

## Acknowledgments

This work was supported in part by US Public Health Service Grants CA-090671, CA-122112 and CA-129186 from the National Cancer Institute, and a Grant from the National Foundation for Cancer Research.

## References

- Shyam K., Penketh P.G., Shapiro M., Belcourt M.F., Loomis R.H., Rockwell S., Sartorelli A.C. (1999) Hypoxia-selective nitrobenzyl-oxycarbonyl derivatives of 1,2-bis(methylsulfonyl)-1-(2-chloroethyl)hydrazines. *J Med Chem*;42:941–946.
- Seow H.A., Penketh P.G., Shyam K., Rockwell S., Sartorelli A.C. (2005) 1,2-Bis(methylsulfonyl)-1-(2-chloroethyl)-2-[[1-(4-nitrophenyl)ethoxy]carbonyl]hydrazine: an anticancer agent targeting hypoxic cells. *Proc Natl Acad Sci USA*;102:9282–9287. PMID: PMC1166587.
- Vaupal P., Harrison L. (2004) Tumor hypoxia: causative factors, compensatory mechanisms, and cellular response. *Oncologist*;9:4–9.
- Moulder J.E., Rockwell S. (1987) Tumor hypoxia: its impact on cancer therapy. *Cancer Metastasis Rev*;5:313–341.
- Vaupel P.W., Frinak S., Bicher H.I. (1981) Heterogeneous oxygen partial pressure and pH distribution in C3H mouse mammary adenocarcinoma. *Cancer Res*;41:2008–2013.
- Green S.L., Giaccia A.J. (1998) Tumor hypoxia and the cell cycle: implications for malignant progression and response to therapy. *Cancer J Sci Am*;4:218–223.
- Bristow R., Hill R (2008) Hypoxia. DNA repair and genetic instability. *Nature*;8:180–192.
- Workman P., Stratford I.J. (1993) The experimental development of bioreductive drugs and their role in cancer therapy. *Cancer Metastasis Rev*;12:73–82.
- Penketh P.G., Shyam K., Sartorelli A.C. (1994) Studies on the mechanism of decomposition and structural factors affecting the aqueous stability of 1,2-bis(sulfonyl)-1-alkylhydrazines. *J Med Chem*;37:2912–2917.
- Penketh P.G., Baumann R.P., Ishiguro K., Shyam K., Seow H.A., Sartorelli A.C. (2008) Lethality to leukemia cell lines of DNA interstrand cross-links generated by cloretazine derived alkylating species. *Leukemia Res*;32:1546–1553. PMID: PMC2888535.
- Bianco P., Haladjian J. (1977) Study of two forms of ferredoxin from *Desulfovibrio gigas* by differential pulse polarography. *Biochem Biophys Res Commun*;78:323–327.
- Baumann R.P., Penketh P.G., Seow H.A., Shyam K., Sartorelli A.C. (2008) Generation of oxygen deficiency in cell culture using a two-enzyme system to evaluate agents targeting hypoxic tumor cells. *Radiation Res*;170:651–660. PMID: PMC2667281.
- Belcourt M.F., Hodnick W.F., Rockwell S., Sartorelli A.C. (1998) The intracellular location of NADH:cytochrome b5 reductase modulates the cytotoxicity of the mitomycins to Chinese hamster ovary cells. *J Biol Chem*;273:8875–8881.
- Zhao Y., Truhlar D.G. (2008) The M06 suite of density functionals for main group thermochemistry, thermochemical kinetics, noncovalent interactions, excited states, and transition elements: two new functionals and systematic testing of four M06-class functionals and 12 other functionals. *Theor Chem Acc*;120:215–241.
- Barone V., Cossi M. (1998) Quantum calculation of molecular energies and energy gradients in solution by a conductor solvent model. *J Phys Chem*;102:1995–2001.
- Cossi M., Rega N., Scalmani G., Barone V. (2003) Energies, structures, and electronic properties of molecules in solution with the C-PCM solvation model. *J Comput Chem*;24:669–681.
- Klamt A., Schüürmann G. (1993) COSMO: a new approach to dielectric screening in solvents with explicit expressions for the screening energy and its gradient. *J Chem Soc Perkin Trans*;2:799–805.

18. Frisch M.J., Trucks G.W., Schlegel H.B., Scuseria G.E., Robb M.A., Cheeseman J.R., Scalmani G. *et al.* (2009) Gaussian 09 Revision A.02. Wallingford, CT: Gaussian, Inc.
19. Lochmüllera C.H., Soute R.W. (1975) Chromatographic resolution of enantiomers : selective review. *J Chromatogr A*;113:283–302.
20. Stoker H.S. (2008) Chapter 18, Carbohydrates, In: Kennedy K. and Berardy R., editors. *General Organic and Biological Chemistry*, 5th edition. Belmont, CA: Brooks/Cole , USA; p. 567–568.
21. Oki M. (1983) Application of dynamic NMR spectroscopy to organic chemistry. *Top Stereochem*;14:1–81.
22. Bringmann G., Mortimer A.J.P., Keller P.A., Gresser M.J., Garner J., Breuning M. (2005) Atroposelective synthesis of axially chiral biaryl compounds. *Angew Chem*;117:5518–5563.
23. Bringmann G., Mortimer A.J.P., Keller P.A., Gresser M.J., Garner J., Breuning M. (2005) Atroposelective synthesis of axially chiral biaryl compounds. *Angew Chem Int Ed*;44:5384–5427.
24. Clayden J., Moran W.J., Edwards P.J., LaPlante S.R. (2009) The challenge of atropisomerism in drug discovery. *Angew Chem Int Ed*;48:6398–6401.
25. Eveleigh P., Hulme E.C., Schudt C., Birdsall N.J. (1989) The existence of stable enantiomers of telenezpine and their stereoselective interaction with muscarinic receptor subtypes. *Mol Pharmacol*;35:477–483.
26. Plusquellic D.F., Pratt D.W. (2007) Probing the electronic structure of peptide bonds using methyl groups. *J Phys Chem A*;111:7391–7397.
27. Wheeler G.P., Bowdon B.J., Grimsley J.A., Lloyd H.H. (1974) Interrelationships of some chemical, physicochemical and biological activities of several 1-(2-haloethyl)-1-nitrosoureas. *Cancer Res*;34:194–200.